

# Cure Kinetics of an Epoxy Resin Containing Naphthyl/Dicyclopentadiene Moieties and Bis-Phenoxy (3-Hydroxy) Phosphine Oxide System and Properties of Its Cured Polymer

Hua Ren,<sup>1,2</sup> Jianzhong Sun,<sup>1</sup> Qian Zhao,<sup>1</sup> Cai Zhiqi,<sup>1</sup> Qincai Ling,<sup>1</sup> Qiyun Zhou<sup>1</sup>

<sup>1</sup>State Key Laboratory of Chemical Engineering, Department of Chemical and Biochemical Engineering, Zhejiang University, Hangzhou 310027, China

<sup>2</sup>College of Material Science and Engineering, Nanjing University of Aeronautics and Astronautics, Nanjing 211100, China

Received 7 November 2007; accepted 21 October 2008

DOI 10.1002/app.29491

Published online 13 January 2009 in Wiley InterScience (www.interscience.wiley.com).

**ABSTRACT:** The cure kinetics of naphthyl/dicyclopentadiene epoxy resin and bisphenoxy (3-hydroxy) phosphine oxide was investigated by differential scanning calorimetry (DSC) under nonisothermal and isothermal condition. The advanced isoconversional method was used to study the nonisothermal DSC data, the effective activation energy of the curing system in the early stage agreed with the value calculated from the Kissinger model and then increased because of the hindrance of molecular mobility. Autocatalytic behavior was shown in the isothermal DSC measurement, which was well described by Kamal model in the early curing stage. In the later stage, a crosslinked network structure

was formed and the curing reaction was mainly controlled by diffusion. The diffusion factor was introduced to optimize the Kamal model and correct the deviation of the calculated data. The physical properties of the cured polymer were evaluated by dynamic mechanical thermal analyses, thermogravimetric analyses, and limiting oxygen index test, which exhibited relatively high glass transition temperature, thermal stability, and flame retardancy. © 2009 Wiley Periodicals, Inc. *J Appl Polym Sci* 112: 761–768, 2009

**Key words:** epoxy resin; bisphenoxy (3-hydroxy) phosphine oxide; cure kinetics

## INTRODUCTION

Epoxy resins have been extensively used in many applications such as coating, adhesives, composite materials, and semiconductor encapsulation because of their electrical and chemical resistance, good mechanical properties, low shrinkage during curing, and great adhesion properties. However, the conventional epoxy resins were seriously confined in some of the applications which require high thermal and flame resistance. Many approaches have been reported for improving the thermal resistance of epoxy resins by changing the structures of the backbone of resins. The introduction of naphthalene ring into the epoxy skeleton is an effective way to increase the glass transition temperature and thermal stability.<sup>1–9</sup> Flame retardancy is another important property of epoxy polymers that should be improved, which is the prime requirement in the applications such as electrochemical uses and advanced composites. Among the different approaches and techniques, organophosphorus compounds have demonstrated ability as flame retard-

ants for thermoplastic and thermoset materials, because the epoxy network could form a thermally stable carbonaceous char on the surface of the burning material during combustion, which acts as a physical barrier to insulate heat from the flame and to prevent further decomposition. Many investigations on developing flame retardant epoxy resins from phosphorus-containing compounds have been reported.<sup>10–12</sup> Moreover, flame retardancy can also be obtained with phosphorus-containing curing agents.<sup>13–15</sup> The incorporation of phosphorus into epoxy systems via curing is an effective and convenient way to improve the flame retardancy. However, the sole high heat resistance or flame retardancy could not satisfy some of the applications such as advanced composites for aerospace industry and new packaging techniques for electronics.

The cure of epoxy resins involves monomers or prepolymers with low molecular weight incorporated into three-dimensional networks. The kinetics of the curing reaction could determine the network morphology, which dictates the physical and mechanical properties of the cured product.<sup>16</sup> Among the several techniques used to study the cure kinetics of epoxy resins, differential scanning calorimetry (DSC) is the most common method to obtain the curing degree and reaction rate, because it

Correspondence to: J. Sun (bigwig@zju.edu.cn).

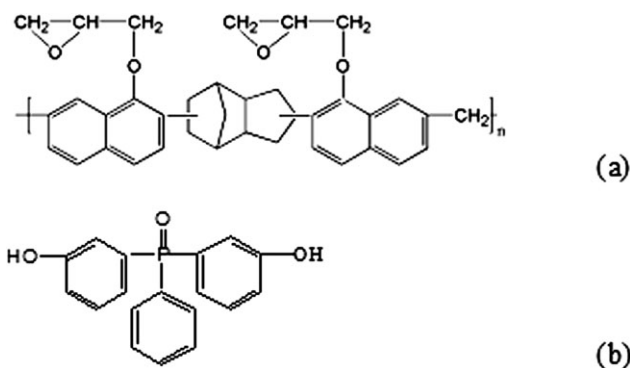
allows the direct measurement of the heat flow which is considered to be proportional to the reaction process. The cure kinetics models are generally developed by analyzing the experimental data obtained from isothermal or dynamic DSC measurement. Kamal's model<sup>17</sup> has been commonly applied to study isothermal DSC curve, a good fit of the experimental data could be found both in early stages and in later diffusion-controlled stages when a diffusion factor was introduced. Kissinger's model<sup>18,19</sup> is a simple and convenient method to calculate the activation energy from nonisothermal DSC measurement. Furthermore, Vyazovkin et al.<sup>20,21</sup> reported a model-free kinetics theory of the advanced isoconventional method (AICM), which associated the changes in the mechanism with changes in the activation energy. The calculated results from these methods help understanding the complex reaction mechanism.

Our previous work had described the synthesis of a novel heat-resistant epoxy resin containing naphthyl/dicyclopentadiene moieties (DCPD).<sup>6</sup> The incorporation of naphthalene ring and dicyclopentadiene group into the epoxy network can improve the thermal stability and glass transition temperature. Additionally, a new phosphorus-containing epoxy resin based on bisphenoxy (2-hydroxy) phenyl phosphine oxide was prepared in our laboratory.<sup>22</sup> The cured resin showed high limiting oxygen index (LOI) values and good thermal stability when cured with 4,4'-diaminodiphenyl sulfone. In this study, the cure kinetics of an epoxy resin containing naphthyl/DCPD moieties and bisphenoxy (3-hydroxy) phosphine oxide (BPHPPO) system was investigated by DSC via isothermal and nonisothermal condition. The values of activation energy calculated from Kamal's model, Kissinger's model, and AICM were compared. The reaction mechanism of the cure was also discussed. Moreover, the thermal and flame-retardant properties of the cured polymer were investigated.

## EXPERIMENTAL METHODS

### Materials

DCPD was obtained from Fluka (Milwaukee, WI). 1-Naphthol (99.0%) from Shanghai Tingxin Chemical Engineering Reagent, China; paraformaldehyde from Tianjin Chemical Reagent, China; epichlorohydrin (ECH) from Acros; phenyl phosphonic dichloride was purchased from Acros; and Resorcinol from Jinlin Reagents, China. Triphenyl phosphine ( $\text{Ph}_3\text{P}$ ) from Shanghai Sanwei was used as a curing accelerator. All solvents and other chemicals were of reagent grade or better and used without further purification.



**Scheme 1** Molecular structure of naphthalene-DCPD epoxy resin (a) and BPHPPO (b).

### Synthesis

#### Preparation of naphthalene-DCPD epoxy resin<sup>6</sup>

The novel epoxy monomer was prepared through Friedel-Crafts condensation between 1-naphthol and DCPD, and then the epoxy monomer reacted with paraformaldehyde and epichlorohydrin orderly to obtain a naphthalene-DCPD epoxy resin.

#### Preparation of BPHPPO<sup>22</sup>

BPHPPO was synthesized from phenyl phosphonic dichloride and resorcinol in a molar ratio of 4.5 : 1. Scheme 1 shows the molecular structure of naphthalene-DCPD epoxy resin and BPHPPO.

### Sample preparation

The naphthalene-DCPD epoxy resin and BPHPPO were mixed in a 1 : 1 equivalent ratio, 0.2 wt % of  $\text{Ph}_3\text{P}$  was mixed as a curing accelerator and some were dissolved in the mixture of *N,N*-dimethylformamide and acetone. Then the mixed solvent was evaporated under vacuum in room temperature and placed in the refrigerator before performing the DSC measurement. The other reactants were heated on hot plates and cured at 120°C for 1 h, 160°C for 1 h, and 240°C for 2 h. Then, cured samples were cooled slowly to room temperature to prevent cracking.

### Characterization

Curing studies were carried out on a Perkin-Elmer DSC-7 under nitrogen atmosphere. The samples were heated from 40 to 300°C at six different rates (5, 8, 10, 12, 15, and 20°C/min) to investigate the dynamic curing procedure. For isothermal cure, samples were sealed in aluminum pans at curing temperature ranging from 175 to 205°C in 10°C increments. At the end of each curing run, the samples were quickly cooled to room temperature and the residual heat of reaction  $\Delta H_r$  was evaluated by

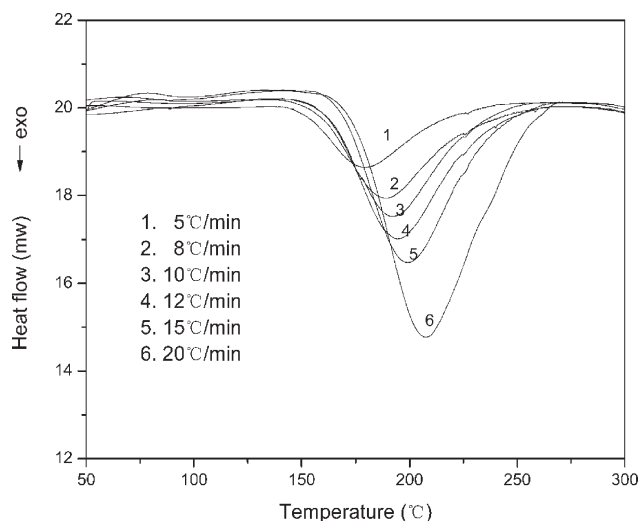


**Figure 1** Dynamic curing DSC curves.

reheating from 40 to 300°C at 20°C/min. The total heat  $\Delta H_o$  evolved during cure is equal to the isothermal heat  $\Delta H_i$  added to  $\Delta H_r$ . Thermogravimetric analysis (TGA) was performed using a Pyris 1 thermogravimetric analyzer (Perkin-Elmer Cetus Instruments, Norwalk, CT) at a heating rate of 10°C/min under nitrogen and air atmosphere. Dynamic mechanical thermal analysis (DMTA) was carried out with a TA DMA Q800 instrument using 2 mm × 10 mm × 30 mm rectangular samples at a programmed heating rate of 3°C/min from 50 to 300°C at a frequency of 1 Hz under air atmosphere. Moisture absorption was tested as follows: 10 mm × 10 mm × 2 mm rectangular samples were dried under vacuum at 120°C for 24 h until trace water had been expelled, then cooling to room temperature, the samples were weighed and placed in 100°C water for 72 h and weighed again. The LOI is the minimum fraction of oxygen in a mixture of oxygen and nitrogen which could just support flaming combustion. The LOI tests were performed according to the testing procedure of ISO4589-1984 with test specimen bar of 7–15 cm in length, 6.5 ± 0.5 mm in width, and 3.0 ± 0.5 mm in thickness. Ten sample bars suspended vertically were ignited by a Bunsen burner. The flame was removed and the timer was started. The concentration of oxygen was raised if the specimen was extinguished before burning for 5 cm in 3 min. The oxygen content was adjusted until the limiting concentration was determined.

## RESULTS AND DISCUSSION

### Nonisothermal kinetic analysis with Kissinger model

Nonisothermal experiments were performed from 40 to 300°C at different heating rates. Figure 1 shows

the dynamic DSC curves of epoxy blend. The kinetic analysis was performed using the Kissinger model.<sup>18,19</sup> According to the Kissinger's method, the activation energy can be obtained from the maximum reaction rate, where at the peak exotherm temperature. The relation could be expressed as the following equation:

$$\frac{d[\ln(q/T_p^2)]}{d(1/T_p)} = \frac{E_a}{R} \quad (1)$$

where  $T_p$  is the peak exotherm temperature,  $q$  is a constant heating rate,  $E_a$  is the activation energy, and  $R$  is the gas constant. Therefore,  $E_a$  could be calculated from slope of the plot of  $\ln(q/T_p^2)$  versus  $1/T_p$  without the need of any assumption about the conversion-dependent equation. Dynamic cure reaction parameters are summarized in Table I.

The Kissinger analysis is based on the relationship between the heating rate and the  $T_p$ . The value of  $E_a$  and  $T_p$  is lower than Naphthalene-DCPD epoxy resin/4,4'-diaminodiphenyl sulfone system (90.9 kJ/mol) with the same analysis method;<sup>6</sup> it may be concluded that the phenolic functional curing agent showed higher reactivity than amino agent. The hydroxyl group of phenol may have more nucleophilicity towards Naphthalene-DCPD epoxy resin.

### Nonisothermal kinetics analysis with AICM

On the basis of the model-free isoconversional methods, changes in the mechanism are associated with changes in the effective activation energy.<sup>20,23,24</sup> These methods used the isoconversional principle that considers that the reaction rate at constant extent of conversion is only a function of the temperature. Compared with other isoconversional methods,<sup>25</sup> AICM of Vyazokin<sup>20</sup> has the merit of decreasing the systematic error to estimate the activation energy. This method has been successfully applied to study the curing process and other complex reaction system including the cure kinetics of a novel combined liquid crystalline epoxy synthesized in our previous work. Without assuming a particular form of reaction model, AICM could be used to

**TABLE I**  
Dynamic Cure Reaction Parameters

Heating rate (°C/min)	$T_o$ (°C)	$T_p$ (°C)	$\Delta H$ (kJ/mol)	$E_a$ (kJ/mol)
5	153.605	179.600	85.348	83.58
8	160.96	189.15	84.925	
10	161.524	191.866	78.659	
12	163.021	194.162	74.870	
15	168.670	199.208	69.962	
20	177.013	208.000	67.844	

evaluate activation energy as a function of the extent of reaction,  $\alpha$ . To associate the heat evolution in the DSC curve with the conversion of the curing reaction, it is necessary to assume that the heat released during the reaction of epoxide groups is the same regardless of the polymer chain with reactive groups increased with the progress of the cure. The heat flow measured by DSC is proportional to the heat release as well as to the cure rate.<sup>26</sup>

$$\frac{dH}{dt} = H_T \frac{d\alpha}{dt} \quad (2)$$

where  $dH/dt$  is the heat flow,  $H_T$  is the heat released calculated from the total exothermal peak area of DSC curve.  $d\alpha/dt$  is the cure rate. The conversion of the curing reaction as a function of time could be obtained from partial integration of the exothermal area under the DSC curve.

$$\alpha = \frac{1}{HT} \int_0^t \left( \frac{dH}{dt} \right) dt \quad (3)$$

By virtue of the assumption that the reaction model is independent of the heating program, the  $J$ -integrals in the range of  $\Delta\alpha$  for any given value of  $\alpha$  are equal for all experiments, regardless of differences in the heating programs. For a series of  $n$  experiments carried out under different temperature programs,  $T_i(t)$ , the activation energy is determined at any particular value of  $\alpha$  by finding  $E_\alpha$ , which minimizes the function,  $\Phi(E_\alpha)$ .<sup>21</sup>

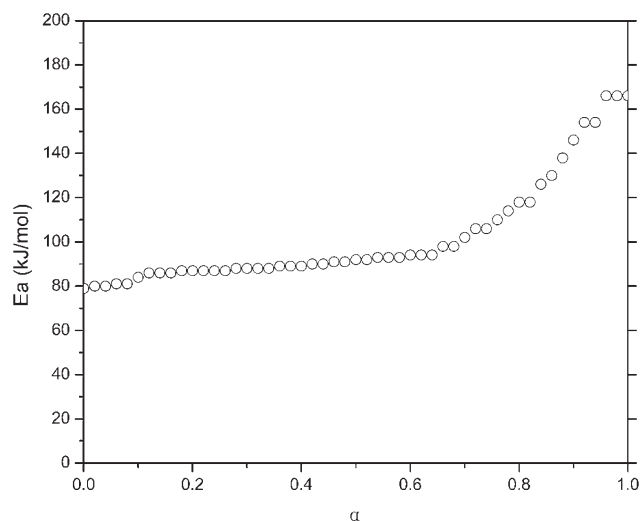
$$\Phi(E_\alpha) = \sum_{i=1}^n \sum_{j \neq i}^n \frac{J[E_\alpha, T_i(t_\alpha)]}{J[E_\alpha, T_j(t_\alpha)]} \quad (4)$$

where the subscripts  $i$  and  $j$  represent ordinal numbers of two experiments performed under different heating programs,  $T_i(t)$ . And the  $J$ -integrals

$$J[E_\alpha, T_i(t_\alpha)] = \int_{t_\alpha - \Delta\alpha}^{t_\alpha} \exp\left(\frac{-E_\alpha}{RT_i(t)}\right) dt \quad (5)$$

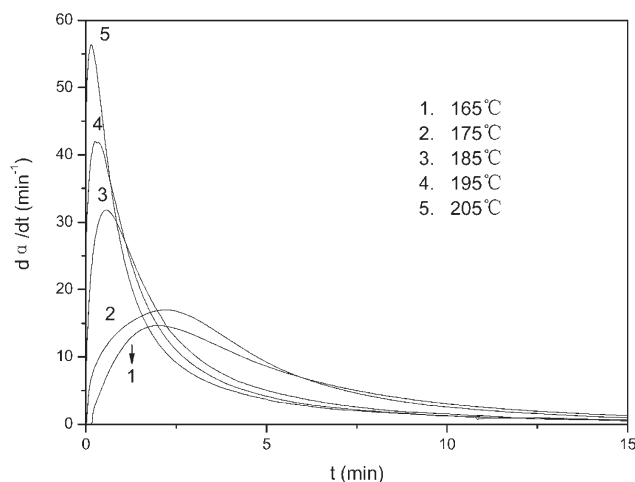
In eq. (5),  $\alpha$  varies from  $\Delta\alpha$  to  $1 - \Delta\alpha$  with a step  $\Delta\alpha = 1/m$ , where  $m$  is the number of intervals chosen for analysis. Because  $m$  is set as 50 in this program,  $\Delta\alpha$  equals to 0.02. The integral,  $J$ , in eq. (5) are evaluated numerically by using the trapezoid rule, with MATLAB toolboxes. The minimization procedure is repeated for each value of  $\alpha$  to find the dependence of the activation energy on the extent of conversion.

Figure 2 shows the variation of effective activation energy with conversion. In the early curing stage ( $\alpha < 0.1$ ), the activation energy is slightly increased from 79 to 84 kJ/mol and then remains almost constant. The decrease in the effective activation energy of epoxy curing is sometimes observed in the early stage and is likely associated with the rate depend-



**Figure 2** Dependence of the effective activation energy on the extent of conversion.

ence on viscosity.<sup>24</sup> However, this phenomenon was not found at the beginning of this curing process and no endothermic peak of the melting before the curing reaction exothermic peak was observed in the nonisothermal DSC curves. The curing system has little change in viscous properties which would cause the change of reaction rate in the early curing stage. In the middle curing stages, activation energy slowly increases to around 94 kJ/mol, autocatalytic reaction mechanism gradually appears. The mobility of the molecules in the curing system becomes difficulty because of the increase of the viscosity in the reaction medium and the growing size of the reactive molecules. Diffusion control effect is another factor to affect the effective activation energy. With the progress of the curing, diffusion rate of the curing system increases and makes the effective activation energy decreased. Both of the two competing mechanism affect the reaction rate simultaneously and autocatalytic reaction mechanism is predominant. In the final curing stages, a significant increase in effective activation energy was observed. Because of the multi-functional structure of naphthalene-DCPD epoxy resin, high crosslinked network was formed and diffusion encountered a larger energy barrier due to the hindrance of the molecular mobility, which leads to higher activation energy of the curing system. Moreover, the  $E_a$ - $\alpha$ -dependency in this study is different from some of the diglycidyl ether of bisphenol A (DGEBA) curing systems reported, the  $E_a$  of which have decreased in the latter curing stages.<sup>27,28</sup> The progress of the cure results in an increase of the glass transition temperature of the epoxy network in the latter curing stages. If the glass transition temperature of the epoxy network rises above the actual experimental temperature of the DSC scan, the mixture of the curing system will



**Figure 3** Curing reaction rates  $d\alpha/dt$  versus time  $t$  at different temperatures.

vitrify to an immobile glass and cause increasing trend of the effective activation energy.<sup>29</sup> In this study, the increase of  $E_a$  could indicate that vitrification occurred in an earlier curing stage than the DGEBA curing systems mentioned above,<sup>27,28</sup> and prove that the conjunction of molecules with multifunctional naphthalene-DCPD structure could facilitate forming an epoxy network with a higher glass transition temperature.

### Isothermal kinetic analysis

Generally, the  $n$ th-order kinetics and autocatalytic kinetics are the two typical reaction mechanisms that describe the thermoset curing reaction.

The  $n$ th-order kinetics<sup>30</sup> could be expressed as

$$\frac{d\alpha}{dt} = k(T)(1 - \alpha)^n \quad (6)$$

The autocatalytic kinetics model by Kamal<sup>17</sup> could be expressed as

$$\frac{d\alpha}{dt} = (k_1 + k_2\alpha^m)(1 - \alpha)^n \quad (7)$$

where  $\alpha$  is the extent of reaction and is calculated from  $\alpha = \Delta H_T / \Delta H_o$ , the partial area under a DSC curve versus time  $t \times k(T)$  is the rate constant at temperature  $T$ ,  $m$  and  $n$  are the reaction orders,  $k_1$  and  $k_2$  are the specific reaction rate constants of Kamal model and follow the Arrhenius relationship:

$$k_i = A_i \exp\left(\frac{-E_i}{RT}\right) \quad (8)$$

$E_i$  could be calculated from slope of the plot of  $\ln k_i$  versus  $T$ .

For  $n$ th-order kinetics model, the maximum reaction rate will be observed at  $t = 0$ , and according to

**TABLE II**  
Isothermal Cure Kinetic Parameters

Temperature (°C)	$k_1$ ( $\times 10^3$ s $^{-1}$ )	$k_2$ ( $\times 10^2$ s $^{-1}$ )	$m$	$n$	$E_1$ (kJ/mol)	$E_2$ (kJ/mol)
165	0.288	0.537	1.10	2.81	80.6	46.4
175	0.495	0.782	0.74	2.77		
185	0.835	1.012	0.71	2.30		
195	1.202	1.266	0.43	2.11		
205	1.863	1.598	0.39	2.02		

the Kamal model, the reaction rate is zero initially and reaches a maximum value at some intermediate conversion.

Figure 3 shows the rate of curing reaction  $d\alpha/dt$  versus time. It was found that the curing reaction rate increased with time during the early curing stage and reached a maximum; Kamal model is suitable for this curing process. A genetic algorithm from MATLAB Toolbox was used to compute the parameters from the experimental data.

The results are shown in Table II.  $k_1$  and  $k_2$  increased with the curing temperature and the corresponding activation energies  $E_1$  and  $E_2$  are 80.6 and 46.4 kJ/mol, respectively. Figure 4 shows the comparisons between the experimental DSC data and the Kamal model with parameters from eq. (7); the kinetic behavior agrees well in early and middle curing stages. However, deviations appear in later curing stage because the mobility of reactive groups is hindered, and the rate of conversion is controlled by diffusion rather than by kinetic factor. The differences could be interpreted by free-volume considerations: the free volume of materials decreased with temperature decreasing and the curing extent increasing, and the rate of diffusion of the reactive

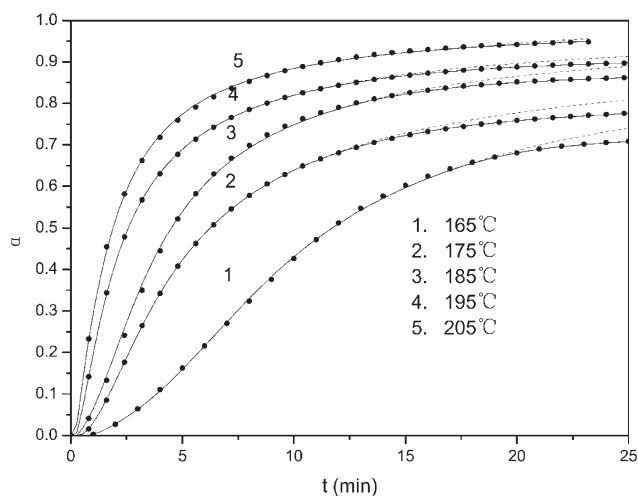


**Figure 4** The plots of the conversion  $\alpha$  versus time  $t$  at different temperatures: (●) experimental data; (---) Kamal model from eq. (7); (—) Autocatalytic model with diffusion factor from eq. (10).

**TABLE III**  
Parameters of Diffusion Factor  $f(\alpha)$

Temperature (°C)	C	$\alpha_c$
165	32.6	0.6925
175	37.9	0.7583
185	60.1	0.8466
195	63.5	0.8913
205	79.0	0.9844

groups was reduced, resulting in the decreasing of curing reaction rate.<sup>31</sup> To characterize the onset of diffusion control effect, a diffusion factor  $f(\alpha)$  could be defined as follows<sup>32,33</sup>:

$$f(\alpha) = \frac{k_e}{k_c} = \frac{1}{1 + \exp[C(\alpha - \alpha_c)]} \quad (9)$$

where  $k_e$  is the overall effective rate constant,  $k_c$  is the rate constant for chemical kinetics, C is a constant, and  $\alpha_c$  is a critical value depended on curing temperature. The values of C and  $\alpha_c$  could be obtained by fitting the modified Kamal model as follows:

$$\frac{d\alpha}{dt} = (k_1 + k_2\alpha^m)(1 - \alpha)^n \frac{1}{1 + \exp[C(\alpha - \alpha_c)]} \quad (10)$$

The parameters of  $f(\alpha)$  were shown in Table III. When the curing reaction is dominated by the kinetic control stage,  $\alpha$  is relatively smaller and the value of  $f(\alpha)$  approximates unity. As  $\alpha$  approaches  $\alpha_c$ ,  $f(\alpha)$  decreases and reaches a value of 0.5 at  $\alpha = \alpha_c$ , and finally approaches zero as the cure effectively stops. Figure 4 shows a comparison between experimental data with those from eq. (10). The calculated results agree well with the original experimental curves both in early and later curing stage.

### Characteristics of the cured polymer

#### TGA

TGA is the most favored technique for rapid evaluation in the thermal stability and degradation behaviors of various polymers. Figures 5 and 6 are the TGA and its differential curves (DTG) of the cured epoxy resin under air and nitrogen atmosphere, respectively. The results indicated that the temperature of 10% degradation of the cured polymer is 367.1°C under nitrogen and 370°C under air. It exhibits a little lower thermal stability than naphthalene-DCPD/4,4'-diaminodiphenyl sulfone cured epoxy resin in the previous study.<sup>6</sup> Although the TGA curves involved distinctly weight loss after the temperature of 10% degradation, more than one peak appeared in DTG curves, implying that the complicated thermal degradation may experience two or

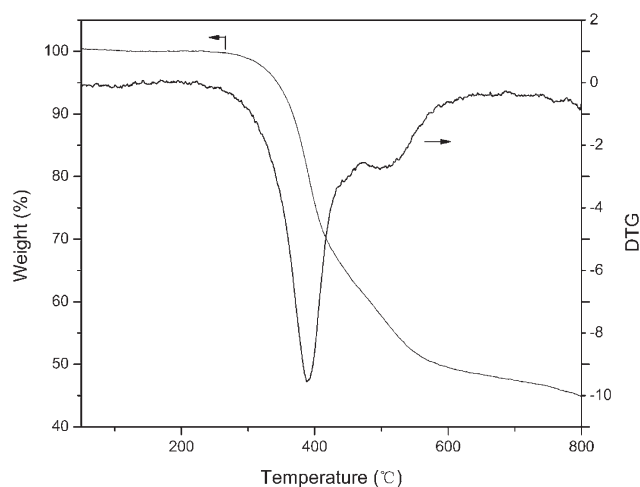


**Figure 5** Weight loss of the cured polymer under nitrogen atmosphere.

three steps. The rapid weight loss temperature is around 400°C in both atmosphere, then the weight loss slowed down. This phenomenon plays an important role in improving the flame retardancy of the materials. The cured resin decomposed and formed a phosphorus-rich residue covered over the surface of the resin to prevent further degradation, raising the decomposition temperature. Even then the weight loss increased again at a higher temperature since 600°C under air atmosphere, the presence of oxygen results in a complicated decomposition mechanism of the cured polymer and the pyrolysis reaction was activated by the existence of oxygen,<sup>34</sup> naphthalene-DCPD/BPHPPPO system exhibits a char yield of 37.1% in air, comparing that of 44.8% in nitrogen. These higher char yields were also important to flame-resistant epoxy systems since high char

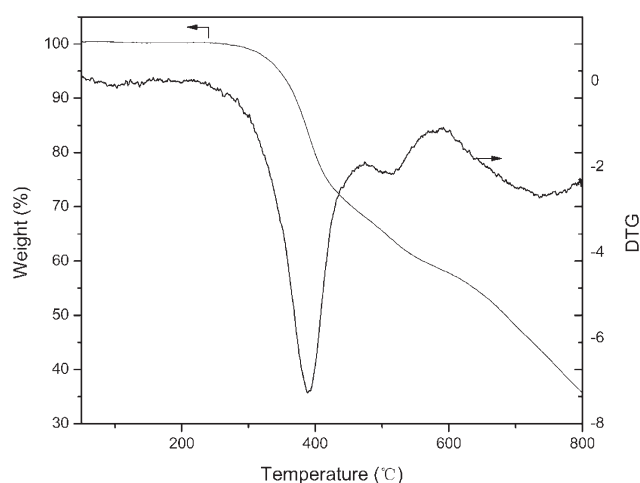


**Figure 6** Weight loss of the cured polymer under air atmosphere.

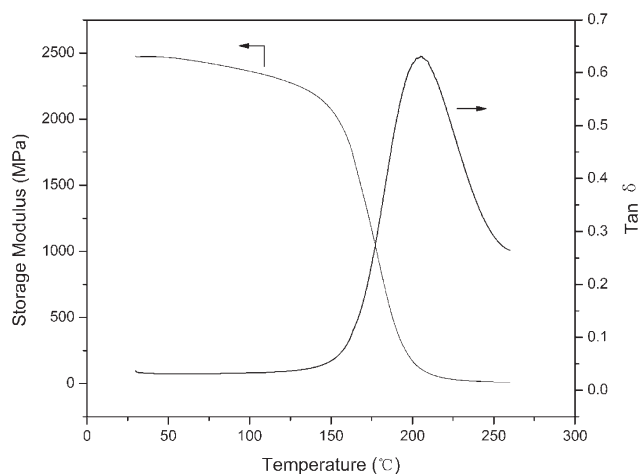


Figure 7 DMTA results of the cured polymer.

yields always lead to high flame retardancy of the phosphorated polymers.

#### Dynamic mechanical thermal analyses

Dynamic mechanical observations were performed to analyze the dynamic elastic modulus and occurrence of molecular mobility transitions such as glass transition.<sup>35</sup> Figure 7 shows the dynamic mechanical thermal analyses (DMTA) scans of the cured epoxy resin. The peak temperature of  $\tan \delta$  was taken as the glass transition temperature. The DMTA measurement indicated that the cured polymer had a  $T_g$  of 205.1°C, which exhibited higher than DGEBA epoxy resins and the phenyl-DCPD epoxy system reported in the literatures.<sup>32,36,37</sup> Glass transition temperature of the cured polymers could rise by introducing the rigid naphthalene group into the molecular backbone, which could restrain the thermal movements and rotations.

#### LOI test of the cured epoxy resin

LOI is defined as the minimum fraction of oxygen from oxygen–nitrogen mixture, which is sufficient to sustain combustion of the specimens after ignition. The value of LOI can be used to evaluate the flame retardant properties of polymers. The flame retardancy of the cured resin was enhanced remarkably by introducing the phosphorus-containing groups into the cured network. The cured Naphthalene-DCPD/BPHPPPO resin has a LOI of 30.5, which is higher than that of traditional flame retardant diglycidyl ether of tetrabromobiphenol A epoxy resin cured with 4,4'-diaminodiphenyl sulfone,<sup>22</sup> indicating that when at a similar molar proportion in the cured resin, the phosphorus element exhibited much better flame retardancy than the bromine element did.

#### Moisture absorption

Moisture absorption will reduce the insulation property of the cured polymer. For a high performance epoxy polymer, it is necessary to decrease the moisture absorption. The moisture absorption was calculated as percent weight gain:

$$\text{Moisture absorption\%} = (W/W_0 - 1) \times 100\%$$

where  $W$  is the weight of sample after dipping in 100°C water for 72 h,  $W_0$  is the weight of sample after placing in vacuum oven for 24 h. The cured polymer exhibited low moisture absorption of 0.966%, the hydrophobic nature of aliphatic DCPD group may be one of the reasons.

#### CONCLUSIONS

The curing characteristics of a epoxy resin containing naphthyl/DCPD moieties with BPHPPPO were investigated by DSC method. In the nonisothermal measurement, the activation energy of curing system calculated from Kissinger model is 83.58 kJ/mol. When using the AICM, a variation of effective activation energy with extent of conversion was observed. The value of  $E_a$  is approximately consistent with that obtained from Kissinger model in the early curing stage and increased in the later stage because molecular mobility was hindered because of the forming of the highly crosslinked network. In the isothermal measurement, the curing system showed autocatalytic behavior and was well described with Kamal model extended with a diffusion factor both in the kinetically controlled stage and diffusion controlled stage. The values of activation energy of  $k_1$  and  $k_2$  are 80.6 and 46.4 kJ/mol, respectively. Furthermore, the high glass transition temperature, LOI, and char yield make the cured polymer a high-performance material having both heat resistant and flame retardant properties.

#### References

1. Kaji, M.; Dndo, T. *J Polym Sci Part A: Polym Chem* 1999, 37, 3063.
2. Duann, Y. F.; Liu, T. M.; Cheng, K. C.; Su, W. F. *Polym Degrad Stab* 2004, 84, 305.
3. Xu, K.; Chen, M. C.; Kui, Z.; Hu, J. W. *Polymer* 2004, 45, 1133.
4. Wang, C. S.; Leu, T. S.; Hsu, K. R. *Polymer* 1998, 39, 2921.
5. Castell, P.; Serra, A.; Galia, M. *J Polym Sci Part A: Polym Chem* 2003, 41, 1536.
6. Ren, H.; Sun, J. Z.; Wu, B. J.; Zhou, Q. Y. *Polymer* 2006, 47, 8309.
7. Lee, J. Y.; Jang, J. J. *J Polym Sci Part A: Polym Chem* 1999, 37, 419.
8. Ochi, M.; Shimizu, Y.; Nakanishi, Y.; Murata, Y. *J Polym Sci Part B: Polym Phys* 1997, 35, 397.
9. Wang, C. S.; Lee, M. C. *Polymer* 2000, 41, 3631.

10. Hergenrother, P. M.; Thompson, C. M.; Smith, J. G. *Polymer* 2005, 46, 5012.
11. Lin, C. H.; Wang, C. S. *Polymer* 2001, 42, 1869.
12. Wang, C. S.; Lin, C. H. *Polymer* 1999, 40, 4387.
13. Jeng, R. J.; Shau, S. M.; Lin, J. J. *Eur Polym J* 2002, 38, 683.
14. Deng, J.; Shi, W. F. *Eur Polym J* 2004, 40, 1137.
15. Wang, C. S.; Shieh, J. Y. *Eur Polym J* 2000, 36, 443.
16. Opalicki, M.; Kenny, M.; Nicolais, L. *J Appl Polym Sci* 1996, 61, 1025.
17. Kamal, M. R. *Polym Eng Sci* 1974, 14, 230.
18. Kissinger, H. E. *J Res Natl Bur Stand* 1956, 57, 217.
19. Kissinger, H. E. *Anal Chem* 1957, 29, 1702.
20. Vyazovkin, S. *J Comput Chem* 2001, 22, 178.
21. Cai, Z. Q.; Sun, J. Z.; Wang, D. D.; Zhou, Q. Y. *J Polym Sci Part A: Polym Chem* 2007, 45, 3922.
22. Ren, H.; Sun, J. Z.; Wu, B. J.; Zhou, Q. Y. *Polym Degrad Stab* 2007, 92, 956.
23. Vyazovkin, S.; Sbirrazzuoli, N. *Macromolecules* 1996, 29, 1867.
24. Vyazovkin, S.; Sbirrazzuoli, N. *Macromol Rapid Commun* 1999, 20, 387.
25. Flynn, J. H. *Thermochim Acta* 1997, 300, 83.
26. Sbirrazzuoli, N.; Mititelu, A.; Vincent, L.; Alizina, C. *Thermochim Acta* 2006, 447, 167.
27. Zhang, Y.; Vyazovkin, S. *Polymer* 2006, 47, 6659.
28. Vyazovkin, S.; Mititelu, A.; Sbirrazzuoli, N. *Macromol Rapid Commun* 2003, 24, 1060.
29. Sbirrazzuoli, N.; Vyazovkin, S. *Thermochim Acta* 2002, 388, 289.
30. Acitelli, M. A.; Prime, R. B.; Sacher, E. *Polymer* 1971, 12, 35.
31. Chern, C. S.; Poehlein, G. W. *Polym Eng Sci* 1987, 27, 788.
32. Cook, W. D.; Simon, G. P.; Burchill, P. J.; Lau, M.; Travis, J. *J Appl Polym Sci* 1997, 64, 769.
33. Cole, K. C.; Hechler, J. J.; Noel, D. *Macromolecules* 1991, 24, 3098.
34. Liu, Y. L.; Hsiue, G. H.; Lee, R. H.; Chiu, Y. S. *J Appl Polym Sci* 1997, 63, 895.
35. Lee, J. Y.; Jang, J.; Hwang, S. S.; Hong, S. M.; Kim, K. U. *Polymer* 1998, 39, 6121.
36. Lin, C. H.; Chiang, J. C.; Wang, C. S. *J Appl Polym Sci* 2003, 88, 2607.
37. Tseng, F. P.; Chang, F. C.; Lin, S. F.; Lin, J. J. *J Appl Polym Sci* 1999, 74, 2196.